Published in final edited form as:
Biomaterials. 2008 March ; 29(9): 1159–1166. doi:10.1016/j.biomaterials.2007.11.020.

The incorporation of poly(lactic-*co*-glycolic) acid nanoparticles into porcine small intestinal submucosa biomaterials

Fadee G. Mondalek[a,b], **Benjamin J. Lawrence**[c], **Bradley P. Kropp**[b], **Brian P. Grady**[a], **Kar-Ming Fung**[d,e], **Sundar V. Madihally**[c], and **Hsueh-Kung Lin**[b,e,*]

[a] Department of Chemical, Biological and Materials Engineering, University of Oklahoma, Norman, OK 73019, USA

[b] Department of Urology, University of Oklahoma Health Sciences Center, Oklahoma City, OK 73104, USA

[c] School of Chemical Engineering, Oklahoma State University, Stillwater, OK 74078, USA

[d] Department of Pathology, University of Oklahoma Health Science Center, Oklahoma City, OK 73104, USA

[e] Department of Veterans Affairs Medical Center, Oklahoma City, OK 73104, USA

Abstract

Small intestinal submucosa (SIS) derived from porcine small intestine has been intensively studied for its capacity in repairing and regenerating wounded and dysfunctional tissues. However, SIS suffers from a large spectrum of heterogeneity in microarchitecture leading to inconsistent results. In this study, we introduced nanoparticles (NPs) to SIS with an intention of decreasing the heterogeneity and improving the consistency of this biomaterial. As determined by scanning electron microscopy and urea permeability, the optimum NP size was estimated to be between 200 nm and 500 nm using commercial monodisperse latex spheres. The concentration of NPs that is required to alter pore sizes of SIS as determined by urea permeability was estimated to be 1 mg/ml 260 nm poly (lactic-*co*-glycolic) acid (PLGA) NPs. The 1 mg/ml PLGA NPs loaded in the SIS did not change the tensile properties of the unmodified SIS or even alter pH values in a cell culture environment. More importantly, PLGA NP modified SIS did not affect human mammary endothelial cells (HMEC-1) morphology or adhesion, but actually enhanced HEMC-1 cell growth.

Keywords

Scaffold; Small intestinal submucosa; Porosity; Nanoparticle; Biocompatibility

1. Introduction

Small intestinal submucosa (SIS) is a xenogenic dense connective tissue harvested from porcine small intestine. The tunica mucosa and the serosa muscularis are mechanically removed from the inner and the outer sides of the intestine, respectively, producing a thin, translucent graft (0.1 mm wall thickness) composed mainly of the submucosal layer of the intestinal wall [1]. SIS is rich in type I collagen and has a resorption rate of 4–16 weeks *in vivo* [2]. SIS is non-immunogenic in over 1000 cross-species transplants with no adverse

*Corresponding author. Department of Urology, University of Oklahoma Health Sciences Center, 920 Stanton L. Young Boulevard, Oklahoma City, OK 73104, USA. Tel.: +1 (405) 271 6900; fax: +1 (405) 271 3118. hk-lin@ouhsc.edu (H.-K. Lin).

response being reported [3,4]. SIS has been investigated to repair and replace a variety of tissues including tendon [5], arterial and venous tissues [1,6,7], skin [8], wound closure [9], as well as urinary bladder [10–12] in a variety of animal models including rodents [13,14], rabbits [15], and dogs [2,16,17].

SIS is superior to synthetic biomaterials because it supports cell ingrowth and differentiation without prior cell seeding such as in the case of bladder regeneration [18]. The superiority of SIS in tissue regeneration may result from intrinsic growth factors [19], glycosaminoglycans, glycoproteins, and proteoglycans [20] residing in SIS that assist in cell migration, proliferation, and differentiation, as well as cell–cell and cell–biomatrix interactions during the regenerative process [21]. However, a number of pre-clinical trials have clearly demonstrated that not all SIS biomaterials are the same. Thus, using SIS is constrained by obtaining reliable, reproducible products in large-scale preparations, and is subjected to the concerns of heterogeneity in its structural features [18].

In order to address the heterogeneity issue related to SIS, we proposed the possibility of altering the microarchitecture of SIS and providing a more uniform SIS for better tissue repair and regeneration using nanotechnology. Biodegradable poly(lactic-*co*-glycolic) acid (PLGA) nanoparticles (NPs) have been manufactured using double emulsification–solvent evaporation method and used as a vehicle for delivering various bioactive molecules including nucleotides [22–24] and drugs [25–27] for therapeutic purposes [28–30].

In this study, we investigated the possibility of modifying SIS using PLGA NPs. NPs modified the SIS porous structure as demonstrated by scanning electron microscopy (SEM) while the membrane's permeability to urea decreased. In addition, NPs did not alter the physical characteristics of the original SIS. More importantly, the NP modified SIS continued to support cell adhesion and proliferation; and cell growth was significantly higher in PLGA NP modified SIS as compared to the unmodified SIS.

2. Materials and methods

2.1. Materials

PLGA with a 50:50 monomer ratio, molecular weight of 106 kDa, and viscosity of 1.05 dl/g was purchased from Absorbable Polymers International (Pelham, AL). Negatively charged polystyrene latex spheres (six sizes between 50 nm and 2000 nm), urea, poly(vinyl alcohol) [PVA], poly(ethyleneimine) [PEI], and MCDB cell culture medium were obtained from Sigma–Aldrich (St. Louis, MO). Single layer SIS (Surgisis®) was obtained from Cook® Biotech (West Lafayette, IN). Chloroform was purchased from EMD Chemicals (San Diego, CA). Urea assay kit was purchased from Diagnostics Chemicals Limited (Oxford, CT). Fetal bovine serum (FBS) and penicillin–streptomycin were obtained from Invitrogen (Carlsbad, CA). Human mammary endothelial cells (HMEC-1) were provided by Dr. Mike Ihnat at the University of Oklahoma Health Sciences Center [31].

2.2. Synthesis of PLGA NPs

PLGA NPs were synthesized using a modified double emulsion solvent evaporation technique [32]. Briefly, 30 mg of PLGA was first dissolved in 1 ml of chloroform. An aliquot of 200 μl of 7% PEI (used to produce positively charged nanoparticles) was added to the PLGA/chloroform solution followed by sonication on ice with a probe sonicator (model VC60; Sonics & Materials, Danbury, CT) set in a continuous mode for 30 s at 100% amplitude. The primary emulsion was transferred into 10 ml of 1% PVA; and the entire solution was sonicated on ice for another 1 min. The organic solvent in the final solution was allowed to evaporate overnight with continuous stirring. PLGA NPs were recovered by centrifugation at 30,000 × *g* for 20 min

at 4°C. The pellet consisting of aggregated NPs was weighed and washed three times with water to remove any residual PVA. PLGA NPs were then resuspended in water using sonication to obtain a final concentration of 2 mg/ml. The NPs were either used immediately or freeze-dried and then stored at −80°C for later use.

2.3. Characterization of PLGA NPs

PLGA NPs were assessed for the particle size, polydispersity index, and zeta potential using diffraction light scattering Zeta PALS (Brookhaven Instruments, Holtsville, NY) at room temperature. Viscosity and refraction indices were set equal to those specific of water. Particle concentration was measured using a FACSCalibur flow cytometer (Becton–Dickinson, San Jose, CA). For this purpose, synthesized NPs were diluted in water at four different concentrations. Particle concentrations were calculated using a calibration curve developed using commercially available latex particles with four different known concentrations.

2.4. Microarchitecture analysis of NP modified SIS

SIS was cut into 1.2 cm × 1.2 cm pieces and assembled in 1.5 ml Eppendorf tubes between the lid and the tube with mucosal side facing upwards. NPs were loaded onto the mucosal side of the SIS inserts. The inserts were incubated overnight at room temperature with a constant shaking on an orbital shaker. To evaluate the microarchitecture of the NP modified SIS, the modified biomatrix was dehydrated using increasing concentrations of ethanol followed by a brief vacuum drying. Samples were then sputter coated with a 15 nm thick layer of gold at 40 mA and analyzed using an SEM (Joel scanning microscope).

2.5. Characterization of physical properties of PLGA NP modified SIS

SIS was converted into wells constructed using silicone glue on the mucosal side; and PLGA NP suspensions with the concentration of 1.273 mg/cm^2 were added onto the mucosal side of SIS. The assembly was placed on an incubator shaker at 37°C overnight. The NP modified SIS membranes were rinsed with water to remove unattached NPs. The thickness of the NP modified SIS was measured using our previously described method [33]. Briefly, the NP modified SIS membranes were cut into small (2 mm × 10 mm) strips. Digital micrographs of the cross section were recorded using an inverted microscope equipped with a CCD camera. The cross section distances were measured using Sigma Scan Pro software (Systat Software, Inc., Point Richmond, CA) which was calibrated using an image of a hemocytometer.

Tensile properties were also determined by our previously described method [33,34]. In brief, 6 cm × 1 cm strips of NP modified SIS membranes were cut from each sample and analyzed using an INSTRON 5842 (INSTRON Inc., Canton, MA) with a constant crosshead speed of 10 mm/min. Tests were performed under hydrated conditions at 37°C using a custom designed chamber.

2.6. Urea permeability studies of NP modified SIS

Permeability was analyzed using the apparatus built in-house as previously described [33]. Briefly, latex spheres and PLGA NPs were suspended in phosphate buffered saline (PBS), and placed on the mucosal side of SIS placed in the permeability chamber. NPs were allowed to settle onto the SIS through gravity on an orbital shaker at 37°C overnight. The NP modified SIS membranes were washed three times with PBS in the chamber, and filled with 550 mM urea (typical concentration at physiological conditions) in PBS. PBS was then added to the serosal side of SIS in the second chamber. Aliquots of samples (20–50 μl) were collected from the second chamber between 0 min and 2 h. Samples collected immediately after the assembly of the chambers were used as time-zero values (i.e. C_2 at $t = 0$). Concentrations of urea were determined using a urea quantitation kit (Diagnostic Chemicals Limited, Oxford, CT).

Membrane permeability was calculated as described previously [33]. In brief, the following equation is obtained using a quasi-steady state approximation

$$\ln\left(\frac{C_0 - 2C_2}{C_0}\right) = -\left(\frac{A_m}{V}P\right)t$$

where C_2 is the concentration of the urea measured at any time t in chamber 2, C_0 (550 mM) is the initial concentration in chamber 1, A_m is the membrane area (3.1416 cm^2 as the radius of the chamber is 1 cm), V is the volume of each chamber (4 ml), and P is the permeability of the matrix. Then $\ln(C_0 - 2C_2)/C_0$ was plotted as a function of time from which the slope $((A_mP)/V)$ was determined using a linear fit. The permeability was calculated using the slope values.

2.7. Evaluation of endothelial cells grown on PLGA NP modified SIS

Endothelial cells were used to determine whether the PLGA NP modified SIS continues to support cell growth or not. SIS was first assembled in Eppendorf tubes and placed in 24-well tissue culture plates as described previously [35]. PLGA NPs were placed onto the mucosal side of the SIS as described above. HMEC-1 were maintained in a complete growth medium (MCDB supplemented with 10% FBS and 1% penicillin–streptomycin) and were seeded at a density of 5.0×10^3 cells/cm^2 on the mucosal side of the SIS. To determine morphologies of HMEC-1 grown on the PLGA NP modified SIS, the cell–SIS constructs were stained with hematoxylin for 30 s, placed on a microscope slide, and sealed with an aqueous mounting medium (Shandon, Pittsburgh, PA).

Genomic DNA contents were quantitated between 3 and 7 days following cell seeding to determine the number of cells grown on NP modified and unmodified SIS. Briefly, cell composite SIS membranes were harvested; and cells were lysed with TNE buffer (10 mM Tris–HCl, pH 8.0, 150 mM NaCl, and 10 mM EDTA) supplemented with 0.2 mg/ml proteinase K (Invitrogen, Carlsbad, CA) at 55°C for 2 h according to our reported procedure [36]. Genomic DNA was subjected to phenol–chloroform extraction, ethanol precipitation, and resolved on 2% agarose gels. Images of the genomic DNA were captured by a gel documentation system (Bio-Rad, Hercules, CA). Genomic DNA band intensities were calculated using the Quantity One® image analysis software (Bio-Rad). Genomic DNA isolated from known numbers of HEMC-1 was run in parallel to construct standard curves.

2.8. Statistical analysis

Statistical differences between two experimental groups were evaluated using student's *t*-test. A statistically significant difference was considered when $p < 0.05$.

3. Results

3.1. Characteristics of synthesized NPs

The average diameter of synthesized PLGA NPs ranged between 162 nm and 306 nm. Polydispersity indices varied from batch to batch, but the value was approximately constant at 0.06. The zeta potential ranged between) 40 mV and + 50 mV, depending on the batch of PLGA NPs synthesized. The morphology of the PLGA NPs as assessed by the SEM showed a porous outer surface (data not shown). The concentration assessment by flow cytometry indicated that 1 mg/ml PLGA NPs suspended in water generated 1.62×10^8 particles/ml.

3.2. Surface structure of NP modified SIS

Commercial nominally monodisperse polystyrene latex spheres (sizes between 50 nm and 2000 nm) were used to determine appropriate sizes of NPs to embed within SIS in order to reduce permeability to urea. Latex spheres with diameters ranging between 200 nm and 500 nm appeared on both mucosal and serosal sides of SIS (Fig. 1C, C′–E, E′). In contrast, larger sizes (1000 nm and 2000 nm) of latex spheres were predominantly present on mucosal side of SIS (Fig. 1A, A′, B and B′), whereas smaller size (50 nm) latex spheres were not observed on either side of SIS (Fig. 1F and F′). These results suggested that NPs smaller than 200 nm could not be retained in SIS; and NPs larger than 500 nm could not fit into the porous structure of SIS.

To determine whether PLGA NPs also possessed similar characteristics as latex spheres, two sizes of PLGA NPs (162 nm and 306 nm) were placed onto the SIS. SEM images demonstrated that both sizes of PLGA NPs (Fig. 2) went through the SIS similar to latex spheres. However, less NPs with 162 nm in size (Fig. 2B) were retained on the mucosal side of SIS as compared to the serosal side (Fig. 2B′). Furthermore, more NPs with 306 nm in size were retained on the mucosal side (Fig. 2C) relative to serosal side (Fig. 2C′). Nevertheless, these results confirmed that NP sizes ranging between 200 nm and 500 nm would be appropriate to fit into the porous structure of SIS.

3.3. The effect of NPs on SIS permeability

NP modified SIS had reduced permeability as compared to unmodified SIS (Fig. 3A). The permeability was 1.13×10^{-3} cm/s in unmodified SIS as compared to 7.71×10^{-4} cm/s in SIS embedded with 200 nm latex sphere. The permeability was reduced further to 6.53×10^{-4} cm/s when 300 nm latex spheres were used as compared to unmodified SIS. When 500 nm latex spheres were used, urea permeability did not show significant reduction from that of unmodified SIS.

The permeability of the SIS to urea was then measured after introducing 260 nm PLGA NPs to SIS. Three different concentrations, 0.1 mg/ml, 1.0 mg/ml, and 5.0 mg/ml of PLGA NPs, were used to determine concentration dependent changes in permeability. The permeability was significantly reduced to 5.63×10^{-4} cm/s when 1.0 mg/ml PLGA NP was used to embed SIS as compared to either 0.1 mg/ml or 5.0 mg/ml PLGA NPs (Fig. 3B).

3.4. The effect of NPs on SIS mechanical properties

To assess the effect of embedding NPs into SIS on its mechanical properties, tensile properties of PLGA NP modified and unmodified SIS were compared. These results showed no significant difference in break stress or break strain (Fig. 4). In addition, when elastic modulus was calculated in the linear range (10–20% strain range), no significant difference was detected between NP modified SIS and unmodified SIS. Both samples showed elastic modulus of 26 MPa, similar to our previous results [33]. However, the thickness of wet SIS in this study averaged 110 μm ± 21 μm as compared to 246 ± 16 μm in our previous study.

3.5. The effect of NPs on cell growth

HMEC-1 grown on both unmodified and NP modified SIS demonstrated similar morphological characteristics as shown in hematoxylin stained cell composite SIS constructs (Fig. 5A). As expected, HEMC-1 adhered and proliferated on unmodified SIS as determined by increasing quantities of genomic DNA contents between days 3 and 7 after cell seeding (Fig. 5B and C). Although HEMC-1 cells adhered equally well on PLGA NP modified SIS as shown by similar genomic DNA contents between NP modified and unmodified SIS on day 3, the number of HEMC-1 was 24,241 ± 3298 on NP modified SIS as compared to 12,336 ± 4971 on unmodified

SIS on day 7 following cell seeding; and the difference was statistically significant ($p < 0.05$) between unmodified SIS and NP modified SIS (Fig. 5C).

4. Discussion

SIS has been intensively investigated for its capability in tissue repair and regeneration in a variety of tissues and animal models in the last 20 years. SIS has been shown to be a promising biomaterial for repairing and regenerating in most applications due to its intrinsic ECM and growth factors [19] that may promote cell migration, growth, and differentiation. Numerous attempts have been made to produce “off-the-shelf” SIS products that would be available for clinical reconstructive surgical procedures [11,12,37,38]. However, SIS suffers from inconsistent results in various applications. These inconsistencies may result from heterogeneities of this biomaterial, since mechanical properties and regenerative capability of SIS depend upon species of animals, ages of animals, and locations of small intestine being used for SIS preparation [33]. The goal of the present work is to introduce NPs to SIS in a hope to provide a consistent quality for this naturally derived biomaterial.

The pores in the SIS are neither uniformly distributed, nor are they uniform in size [33]. This explains the wide size ranges (200–500 nm) of particles capable of embedding themselves in SIS. The absence of small size NPs (50 nm) within SIS in the SEM images may result from two reasons. First, 50 nm latex particles may be too small to be retained in SIS in the SEM images; or, second, the 15 nm gold used for coating during SEM procedures may make the particles difficult or impossible to be distinguished from the SIS. It is also important to note that SIS differs from batch to batch from the same manufacturer. For example, previously we reported Cook SIS thickness as 101 μm ± 19.84 μm (dry) and 246 μm ± 16.22 μm (wet) [33]. In the present study, thickness of the Cook SIS was 29.6 μm ± 6.4 μm (dry) and 110 μm ± 21 μm (wet). Based on the inconsistency of the SIS and the wide variation in pore size, a combination of different sizes of NPs might ultimately be needed to achieve maximal uniformity of SIS.

Permeability studies indicated that there was no statistically significant difference between the unmodified SIS and 200 nm latex spheres modified SIS, or between the unmodified SIS and 500 nm latex spheres embedded SIS. In contrast, a significant difference was detected between the unmodified SIS and 300 nm NP modified SIS. It appeared that the 200 nm NPs plugged some of the SIS pores as observed in the SEM images (Fig. 1), and perhaps resulted in a slight reduction in permeability. However, the particles may not fill a critical number of the pores to provide a statistically significant reduction in permeability. The same explanation can be applied to 500 nm NPs. In contrast, 300 nm latex spheres seem to fill enough number of pores in SIS to provide a significant reduction in permeability. It may also be possible to further reduce the permeability of SIS if a combination of different sizes of NPs is used for SIS modification.

To determine the minimal concentration of PLGA NPs that can modify SIS, 260 nm PLGA NPs were used in urea permeability assays. With 1 mg/ml PLGA NPs, the permeability was reduced significantly as compared to unmodified SIS. The failure of a higher concentration, 5 mg/ml, to significantly reduce SIS permeability might result from aggregation of this concentration of PLGA NPs; and these aggregates were too large to fit into the porous structure of SIS and hence could not reduce SIS permeability as seen with larger sizes of latex spheres (1 μm and 2 μm).

Reduction in SIS permeability may be a critical factor in determining the success of tissue repair and regeneration especially in bladder regeneration. Based on our observation, proximal sections of SIS are more permeable to urea than distal sections of SIS [33], and have not been

successful for bladder regeneration [18]. The leakage of urine in augmented bladder can have detrimental effects on inflammatory responses during the process toward complete regeneration, and may result in the absence of bladder regeneration as we reported in a dog bladder augmentation model [18]. We expect that the reduction in permeability in NP modified SIS may significantly improve tissue regeneration processes particularly in urinary bladder regeneration.

Lactic acid and glycolic acid are PLGA particles degradation products. One major concern of using PLGA NPs in tissue engineering is that these products might alter the microenvironments and interfere with cell physiology. When PLGA NP modified SIS was placed in 37°C humidified incubator for a period 7 days in the complete growth medium, there was no detectible change in pH values (data not shown). This result indicated that the products generated during PLGA degradation may not have adverse effects on cell physiology.

The most intriguing observation was that PLGA NP modified SIS continues to support cell adhesion and growth. Since SIS interferes with various assay systems including colometric-based, fluorescence-based, and ^{3}H-thymidine incorporation assays for determining cell proliferation (data not shown), these assays are not appropriate for quantitating *in vitro* cell growth on SIS. In this study, the number of cells growing on SIS was estimated by quantitating the amounts of extractible genomic DNA. PLGA NP modified SIS did not interfere with HEMC-1 adhesion as demonstrated by the similar quantity of genomic DNA extracted from both unmodified and modified SIS on day 3. HEMC-1 grew gradually on unmodified SIS between days 3 and 7 as we expected. Interestingly, HEMC-1 proliferation was significantly higher on PLGA NP modified SIS as compared to unmodified SIS on day 7. The mechanism that is responsible for the enhanced cell proliferation in PLGA NP modified SIS is not clear. The elevated cell proliferation might result from a uniform porous structure provided by NP modified SIS for easier cell migration and distribution, or synergistic effects of PLGA and SIS to support cell growth [39–41].

5. Conclusion

Heterogeneity of SIS presents a major issue for this biomaterial to produce consistent tissue repair and regeneration. We demonstrated that the introduction of NPs represents a potential solution to improve the quality of regenerated tissues using SIS. The elevated HEMC-1 cell proliferation on PLGA NP modified SIS may result from uniform porous structure as compared to unmodified SIS, and may translate to enhanced angiogenesis *in vivo*.

Acknowledgments

This work was funded by the Oklahoma Center for Advancement of Science and Technology (HR05-075) and National Institutes of Health (1R21DK074858-01A2) to S.V.M.

Abbreviations

SIS	small intestinal submucosa
PLGA	poly(lactic-*co*-glycolic) acid
NPs	nanoparticles
EC	endothelial cells
ECM	extracellular matrix
PVA	poly(vinyl alcohol)
PEI	poly(ethyleneimine)

PBS	phosphate buffer saline
TNE	Tris–HCl/NaCl/EDTA
HMEC	human mammary endothelial cells

References

1. Badylak SF, Lantz GC, Coffey A, Geddes LA. Small intestinal submucosa as a large diameter vascular graft in the dog. J Surg Res 1989;47(1):74–80. [PubMed: 2739401]
2. Badylak SF, Kropp B, McPherson T, Liang H, Snyder PW. Small intestinal submucosa: a rapidly resorbed bioscaffold for augmentation cystoplasty in a dog model. Tissue Eng 1998;4(4):379–87. [PubMed: 9916170]
3. Kropp BP. Small-intestinal submucosa for bladder augmentation: a review of preclinical studies. World J Urol 1998;16(4):262–7. [PubMed: 9775425]
4. Paterson RF, Lifshitz DA, Beck SD, Siqueira TM Jr, Cheng L, Lingeman JE, et al. Multilayered small intestinal submucosa is inferior to autologous bowel for laparoscopic bladder augmentation. J Urol 2002;168(5):2253–7. [PubMed: 12394770]
5. Androjna C, Spragg RK, Derwin KA. Mechanical conditioning of cell-seeded small intestine submucosa: a potential tissue-engineering strategy for tendon repair. Tissue Eng 2007;13(2):233–43. [PubMed: 17518560]
6. Lantz GC, Badylak SF, Coffey AC, Geddes LA, Sandusky GE. Small intestinal submucosa as a superior vena cava graft in the dog. J Surg Res 1992;53(2):175–81. [PubMed: 1405606]
7. Lantz GC, Badylak SF, Coffey AC, Geddes LA, Blevins WE. Small intestinal submucosa as a small-diameter arterial graft in the dog. J Invest Surg 1990;3(3):217–27. [PubMed: 2078544]
8. Kim MS, Hong KD, Shin HW, Kim SH, Kim SH, Lee MS, et al. Preparation of porcine small intestinal submucosa sponge and their application as a wound dressing in full-thickness skin defect of rat. Int J Biol Macromol 2005;36(1–2):54–60. [PubMed: 15939465]
9. Clarke KM, Lantz GC, Salisbury SK, Badylak SF, Hiles MC, Voytik SL. Intestine submucosa and polypropylene mesh for abdominal wall repair in dogs. J Surg Res 1996;60(1):107–14. [PubMed: 8592400]
10. Caione P, Capozza N, Zavaglia D, Palombaro G, Boldrini R. In vivo bladder regeneration using small intestinal submucosa: experimental study. Pediatr Surg Int 2006;22(7):593–9. [PubMed: 16773371]
11. Zhang Y, Kropp BP, Lin HK, Cowan R, Cheng EY. Bladder regeneration with cell-seeded small intestinal submucosa. Tissue Eng 2004;10(1–2):181–7. [PubMed: 15009944]
12. Colvert JR 3rd, Kropp BP, Cheng EY, Pope JCt, Brock JW 3rd, Adams MC, et al. The use of small intestinal submucosa as an off-the-shelf urethral sling material for pediatric urinary incontinence. J Urol 2002;168(4 Pt 2):1872–5. [discussion 5–6]. [PubMed: 12352379]
13. Prevel CD, Eppley BL, Summerlin DJ, Sidner R, Jackson JR, McCarty M, et al. Small intestinal submucosa: utilization as a wound dressing in full-thickness rodent wounds. Ann Plast Surg 1995;35 (4):381–8. [PubMed: 8585681]
14. Vaught JD, Kropp BP, Sawyer BD, Rippy MK, Badylak SF, Shannon HE, et al. Detrusor regeneration in the rat using porcine small intestinal submucosal grafts: functional innervation and receptor expression. J Urol 1996;155(1):374–8. [PubMed: 7490890]
15. Gubbels SP, Richardson M, Trune D, Bascom DA, Wax MK. Tracheal reconstruction with porcine small intestine submucosa in a rabbit model. Otolaryngol Head Neck Surg 2006;134(6):1028–35. [PubMed: 16730551]
16. Kropp BP, Rippy MK, Badylak SF, Adams MC, Keating MA, Rink RC, et al. Regenerative urinary bladder augmentation using small intestinal submucosa: urodynamic and histopathologic assessment in long-term canine bladder augmentations. J Urol 1996;155(6):2098–104. [PubMed: 8618344]
17. Kropp BP, Sawyer BD, Shannon HE, Rippy MK, Badylak SF, Adams MC, et al. Characterization of small intestinal submucosa regenerated canine detrusor: assessment of reinnervation, in vitro compliance and contractility. J Urol 1996;156(2 Pt 2):599–607. [PubMed: 8683741]

18. Kropp BP, Cheng EY, Lin HK, Zhang Y. Reliable and reproducible bladder regeneration using unseeded distal small intestinal submucosa. J Urol 2004;172(4 Pt 2):1710–3. [PubMed: 15371796]
19. Cheng EY, Kropp BP. Urologic tissue engineering with small-intestinal submucosa: potential clinical applications. World J Urol 2000;18(1):26–30. [PubMed: 10766040]
20. Pu LL. Small intestinal submucosa (surgisis) as a bioactive prosthetic material for repair of abdominal wall fascial defect. Plast Reconstr Surg 2005;115(7):2127–31. [PubMed: 15923867]
21. Ho KL, Witte MN, Bird ET. 8-Ply small intestinal submucosa tension-free sling: spectrum of postoperative inflammation. J Urol 2004;171(1):268–71. [PubMed: 14665891]
22. Yi F, Wu H, Jia GL. Formulation and characterization of poly (D,L-lactide-*co*-glycolide) nanoparticle containing vascular endothelial growth factor for gene delivery. J Clin Pharm Ther 2006;31(1):43–8. [PubMed: 16476119]
23. Shakweh M, Fattal E. Design and characterisation of poly(lactide-*co*-glycolide) small particulate systems for the delivery of immunostimulant CpG oligonucleotide. J Nanosci Nanotechnol 2006;6 (9–10):2811–20. [PubMed: 17048487]
24. Hillaireau H, Le Doan T, Couvreur P. Polymer-based nanoparticles for the delivery of nucleoside analogues. J Nanosci Nanotechnol 2006;6(9–10):2608–17. [PubMed: 17048470]
25. Zweers MLT, Engbers GHM, Grijpma DW, Feijen J. Release of anti-restenosis drugs from poly (ethylene oxide)-poly (DL-lactic-*co*-glycolic acid) nanoparticles. J Control Release 2006;114(3): 317–24. [PubMed: 16884807]
26. Musumeci T, Ventura CA, Giannone I, Ruozi B, Montenegro L, Pignatello R, et al. PLA/PLGA nanoparticles for sustained release of docetaxel. Int J Pharm 2006;325(1–2):172–9. [PubMed: 16887303]
27. Leo E, Scatturin A, Vighi E, Dalpiaz A. Polymeric nanoparticles as drug controlled release systems: a new formulation strategy for drugs with small or large molecular weight. J Nanosci Nanotechnol 2006;6(9–10):3070–9. [PubMed: 17048520]
28. Wendorf J, Singh M, Chesko J, Kazzaz J, Soewanan E, Ugozzoli M, et al. A practical approach to the use of nanoparticles for vaccine delivery. J Pharm Sci 2006;95(12):2738–50. [PubMed: 16927245]
29. Lamprecht A, Koenig P, Ubrich N, Maincent P, Neumann D. Low molecular weight heparin nanoparticles: mucoadhesion and behaviour in caco-2 cells. Nanotechnology 2006;17(15):3673–80.
30. Farokhzad OC, Cheng JJ, Teply BA, Sherifi I, Jon S, Kantoff PW, et al. Targeted nanoparticle–aptamer bioconjugates for cancer chemotherapy in vivo. Proc Natl Acad Sci U S A 2006;103(16): 6315–20. [PubMed: 16606824]
31. Ades EW, Candal FJ, Swerlick RA, George VG, Summers S, Bosse DC, et al. Hmec-1: establishment of an immortalized human microvascular endothelial cell line. J Invest Dermatol 1992;99(6):683–90. [PubMed: 1361507]
32. Astete CE, Sabliov CM. Synthesis and characterization of PLGA nanoparticles. J Biomater Sci Polym Ed 2006;17(3):247–89. [PubMed: 16689015]
33. Raghavan D, Kropp BP, Lin HK, Zhang Y, Cowan R, Madihally SV. Physical characteristics of small intestinal submucosa scaffolds are location-dependent. J Biomed Mater Res A 2005;73(1):90–6. [PubMed: 15693016]
34. Sarasam A, Madihally SV. Characterization of chitosan–polycaprolactone blends for tissue engineering applications. Biomaterials 2005;26(27):5500–8. [PubMed: 15860206]
35. Mondalek FG, Zhang YY, Kropp B, Kopke RD, Ge X, Jackson RL, et al. The permeability of SPION over an artificial three-layer membrane is enhanced by external magnetic field. J Nanobiotechnology 2006;4:4. [PubMed: 16603066]
36. Selvakumaran M, Lin HK, Sjin RT, Reed JC, Liebermann DA, Hoffman B. The novel primary response gene *myd118* and the proto-oncogenes *myb*, *myc*, and *bcl-2* modulate transforming growth factor beta 1-induced apoptosis of myeloid leukemia cells. Mol Cell Biol 1994;14(4):2352–60. [PubMed: 8139540]
37. Kropp BP, Cheng EY, Pope JCt, Brock JW 3rd, Koyle MA, Furness PD 3rd, et al. Use of small intestinal submucosa for corporal body grafting in cases of severe penile curvature. J Urol 2002;168 (4 Pt 2):1742–5. [discussion 5]. [PubMed: 12352349]

38. Kropp BP, Eppley BL, Prevel CD, Rippy MK, Harruff RC, Badylak SF, et al. Experimental assessment of small intestinal submucosa as a bladder wall substitute. Urology 1995;46(3):396–400. [PubMed: 7660517]

39. Bhang SH, Lim JS, Choi CY, Kwon YK, Kim BS. The behavior of neural stem cells on biodegradable synthetic polymers. J Biomater Sci Polym Ed 2007;18(2):223–39. [PubMed: 17323855]

40. Pattison MA, Wurster S, Webster TJ, Haberstroh KM. Three-dimensional, nano-structured PLGA scaffolds for bladder tissue replacement applications. Biomaterials 2005;26(15):2491–500. [PubMed: 15585251]

41. Pattison M, Webster TJ, Leslie J, Kaefer M, Haberstroh KM. Evaluating the in vitro and in vivo efficacy of nano-structured polymers for bladder tissue replacement applications. Macromol Biosci 2007;7(5):690–700. [PubMed: 17477448]

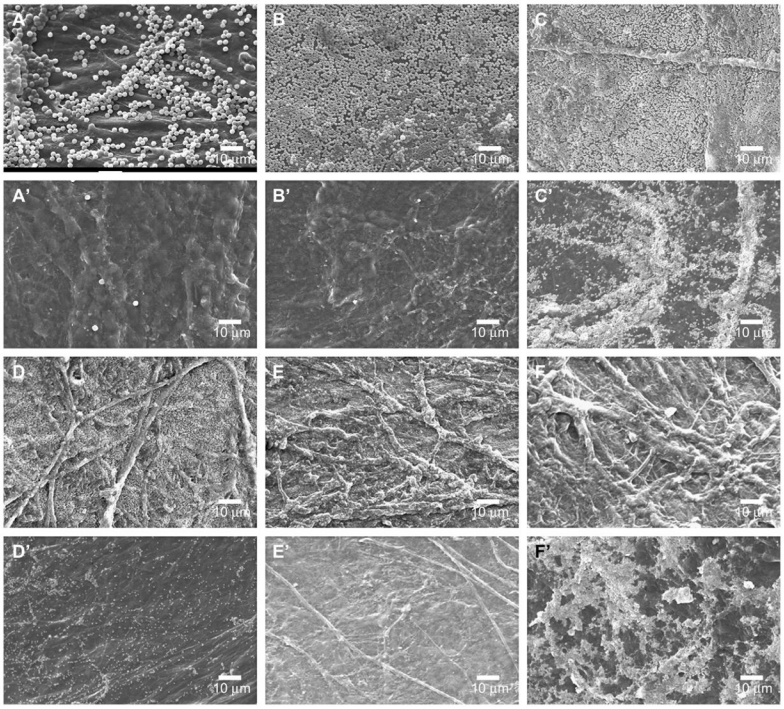

Fig. 1.

SEM images of latex spheres modified SIS. Mucosal sides of SIS were imaged following overnight embedding of 2 μm (A), 1 μm (B), 500 nm (C), 300 nm (D), 200 nm (E), and 50 nm (F) latex spheres. Serosal sides of the same SIS membranes were also imaged (A′–F′).

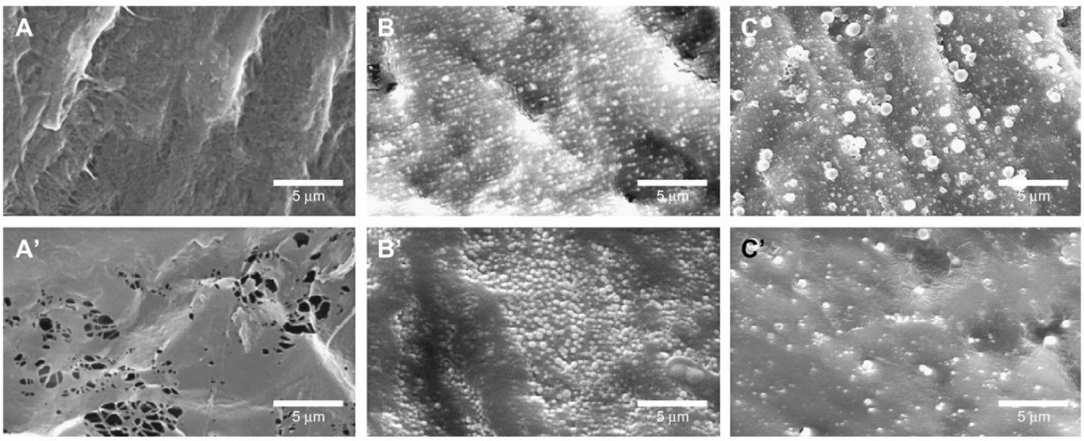

Fig. 2.

SEM images of PLGA NP modified SIS. Unmodified SIS was imaged on mucosal side (A) and serosal side (A′). Following 162 nm PLGA NPs embedding, mucosal side (B) and serosal side (B′) of the SIS structure were shown. Panels C and C′ show SIS modified by 306 nm PLGA NPs on mucosal and serosal sides of SIS, respectively.

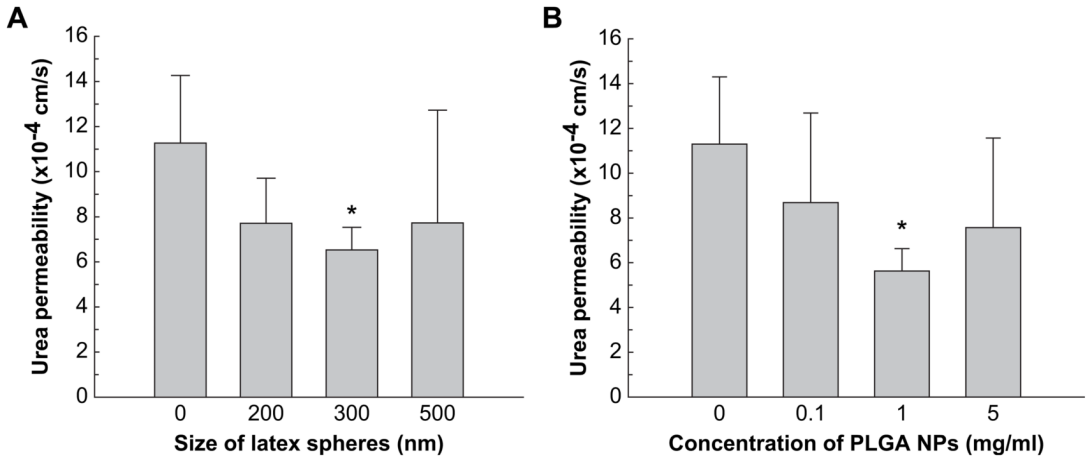

Fig. 3.

Alteration of SIS permeability to urea by NPs. Permeability chambers were set up by placing latex spheres (A) or PLGA NPs (B) on the mucosal side of SIS to demonstrate size-dependent and concentration dependent permeability, respectively. Zero size or zero concentration indicates permeability measured with unmodified SIS, i.e. no spheres. Results are present as mean ± standard deviation from three independent experiments. * Indicates that these results were different vs. unmodified SIS ($p < 0.05$).

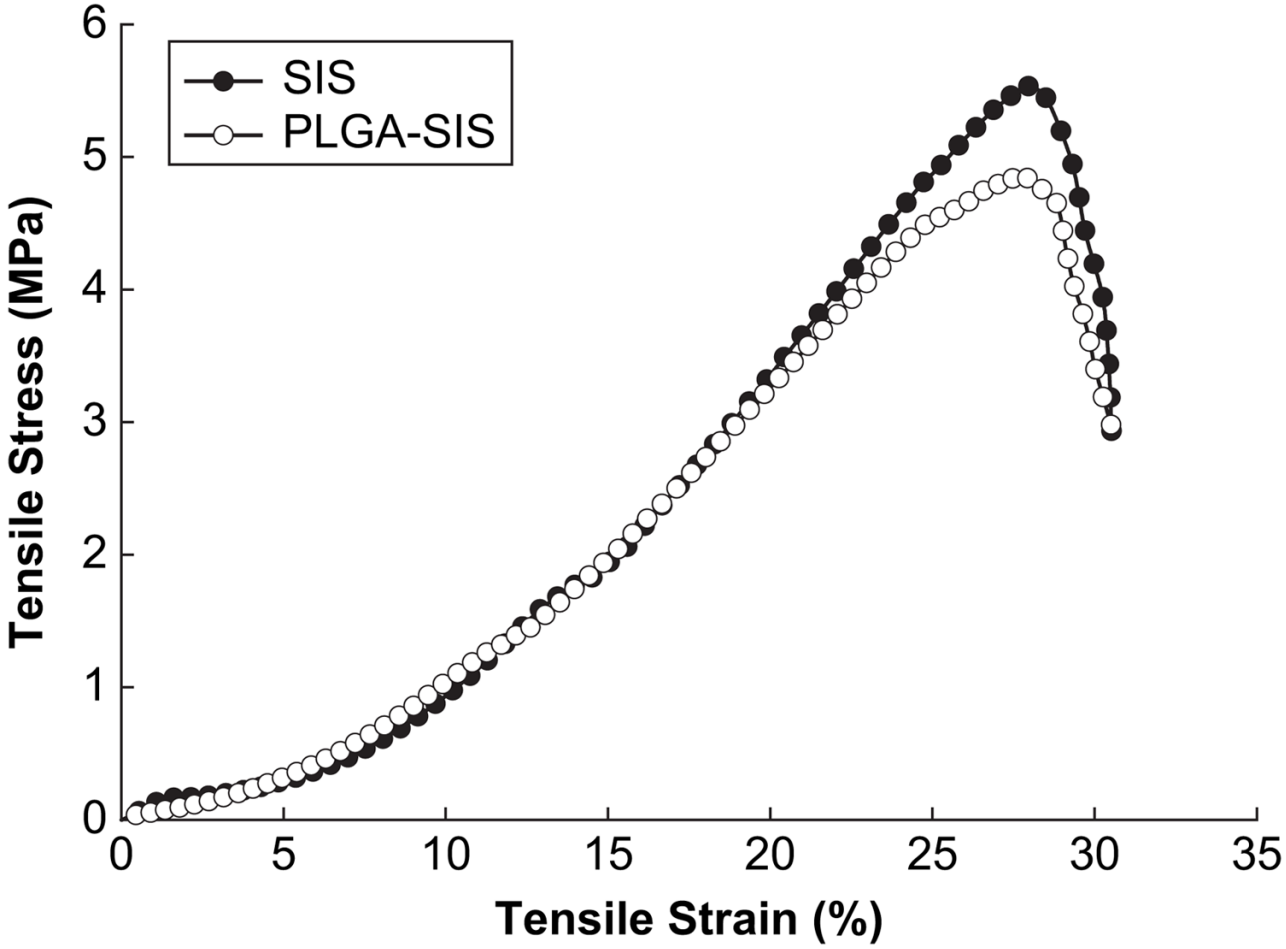

Fig. 4.
Stress–strain curves of SIS with and without PLGA NPs.

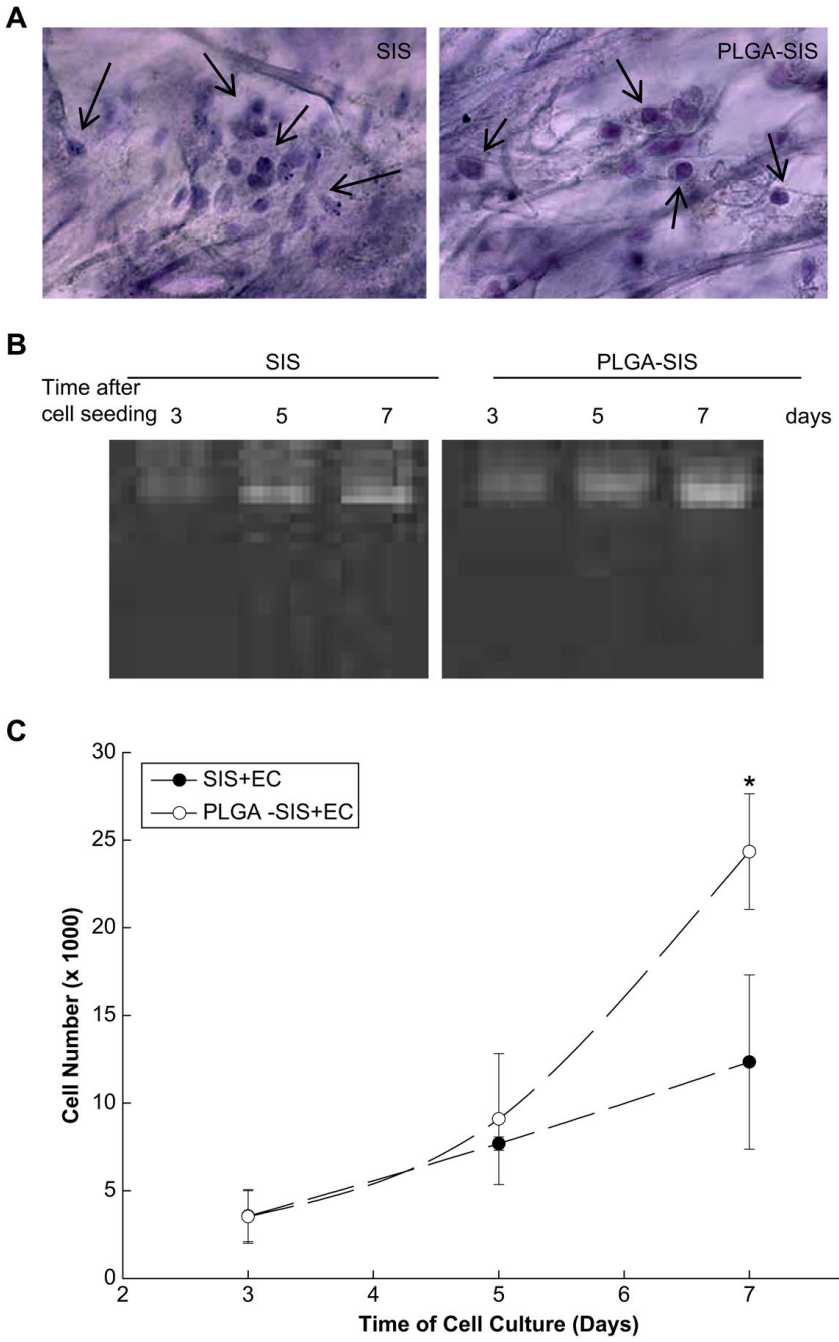

Fig. 5.

Endothelial cell growth on PLGA NP modified SIS. (A) Morphological presentation of HEMC-1 cells on unmodified SIS and PLGA NP modified SIS. Arrows indicate the presence of cells in SIS structure. (B) HEMC-1 proliferation on SIS as determined by genomic DNA contents was presented over a period of 7 days following cell seeding. (C) Quantitative presentation of HEMC-1 growth on SIS. Results were presented as mean ± standard deviation of cell numbers from three independent experiments. * Indicates the results were different vs. unmodified SIS on day 7 ($p < 0.05$).